



The diffusion behavior of carbon in sputtered tungsten film and sintered tungsten block and its effect on diamond nucleation and growth



Taimin Yang^a, Qiuping Wei^{a,b,*}, Yao Qi^a, Zhiming Yu^{a,**}

^a School of Materials Science and Engineering, Central South University, Changsha 410083, PR China

^b State Key Laboratory of Powder Metallurgy, Central South University, Changsha 410083, PR China

ARTICLE INFO

Article history:

Received 12 November 2014

Received in revised form 18 December 2014

Accepted 20 December 2014

Available online 26 December 2014

Keywords:

Diffusion

Diamond films

HFCVD

Sputtered tungsten films

Nucleation surface

Ultra-smooth

ABSTRACT

Diamond was done on sintered tungsten block with or without sputtered tungsten films. The effects of various depositing conditions, including methane concentration, temperature, pressure, the diamond seeding step and reaction time, on diamond growth were investigated in detail. The results show that the sputtered tungsten film has a dual effect on diamond growth. Firstly, after ultrasonication with diamond slurry, the tungsten film will adsorb a large number of diamond nanoparticles. Therefore, the nucleation density of diamond will be substantially improved. Secondly, the film will be carbonized during the deposition process and the carbon on the surface of the film will decrease. Methane concentration generally does not affect the carbonization level of the tungsten film but higher temperature will lead to a higher level of carbonization. The carbonization process of sputtered tungsten films during deposition is made up of two steps. Also, the nucleation surface of diamond was revealed. The nucleation surface was a layer of ultrasmooth and seamless nanocrystalline diamond film with high-quality and special surface architecture (tiny peaks arrays), which is potential to be applied in MEMS and field-emission devices. A potential method to prepare ultrasmooth nanocrystalline diamond films is proposed.

© 2014 Elsevier B.V. All rights reserved.

1. Introduction

Diamond has been regarded as a precious material for centuries and it has many good properties, such as extreme hardness, low friction coefficient, chemical stability, wide band gap, negative surface emission energy, the highest thermal conductivity [1] and good biocompatibility [2]. Therefore, diamond is a very attractive material for a large number of applications, including cutting tools [3,4], artificial joints [5,6], thermal conductors [7,8], field-emission devices [9] and MEMS [10,11].

During chemical vapor deposition (CVD) of diamond films, some substrates (W, Mo, Ta, etc.) are likely to form an interfacial carbide layer, which serves as a buffer layer. The buffer layer limits carburization (the dissolution of activated carbon source into the substrate) and relieves the stress at the interface [12]. Among these substrates, tungsten is one of the best substrates for diamond growth because of the low thermal expansion mismatch between tungsten and diamond. So the diamond film coated tungsten blocks are used as electrodes to degrade organic substance in sewage [13]. Researchers also prepared boron-

doped diamond films on tungsten wires to produce diamond micro-electrodes, which have remarkable electrochemistry properties [14,15]. Others deposited diamond films on tungsten wires and then corroded the core to prepare diamond micro-tubes [16–18]. These diamond micro-tubes can be used in microfluidic applications [19,20].

On the other hand, it is difficult to grow diamond on substrates containing iron group elements (Fe, Co, Ni). These elements have high solubility of carbon. Diamond can hardly nucleate on these substrates. Also, these substrates can serve as catalysts for graphite formation during the CVD process, making diamond nucleation even difficult [21–23]. To solve this problem, tungsten was deposited on these substrates as an interlayer before diamond preparation [24]. The tungsten interlayer can enhance the nucleation density and surface coverage and reduce the surface roughness for micro/nano crystalline diamond (MCD/NCD) films. Many articles proved that the interlayer enhanced the nucleation density of diamond dramatically [25] and this technique was a potential way to produce ultra-smooth nanocrystalline diamond films for MEMS and field-emission applications. Buijnsters and co-workers examined diamond growth on six different metallic sputtered seed nanolayers (Cr, Mo, Nb, Ti, V and W). They found that the highest seed density of diamond nanoparticles anchored to the metallic (W) surface [26]. Also, the tungsten interlayer will shield the adverse impact of the substrates. Therefore, diamond films with good quality and adhesion were prepared on tungsten-coated steel substrates [27] and tungsten-coated

* Correspondence to: Q. Wei, School of Materials Science and Engineering, Central South University, Changsha 410083, PR China. Tel.: +86 731 8830335; fax: +86 731 8876692.

** Corresponding author. Tel.: +86 731 8830335; fax: +86 731 8876692.
E-mail addresses: qpwei@csu.edu.cn (Q. Wei), zhiming@csu.edu.cn (Z. Yu).

WC–Co substrates [28]. Another benefit of sputtered interlayer is that it provides a new way to prepare ultrasmooth nanocrystalline diamond films. This was proved to be quite effective using Mo interlayers [29,30].

The published literatures mainly focused on the effect of interlayer on adhesion, diamond nucleation and surface roughness after diamond deposition. But the diffusion behavior of interlayer and its influence on nucleation and surface morphology did not receive enough attention. Also, the phase transformation and the reaction process of tungsten and carbon during HFCVD are not fully understood. In this paper, the diffusion behavior of carbon in tungsten interlayer and its effects under the different methane concentration, pressure, growing time and pretreatment methods are discussed. Unlike regular pretreatment procedures, most of the sputtered substrates used in the experiment were not submerged into diamond powder slurry in order to eliminate the influence of adsorbed diamond particles. The impacts of various deposition parameters on the surface morphology and growth rate of diamond films were investigated by field emission scanning electron microscope (FE-SEM), X-ray diffraction (XRD), focused ion beam (FIB), STEM and Raman spectroscopy. The composition of the tungsten film was analyzed in detail. The results show that the tungsten interlayer has a dual effect. With diamond ultrasonic agitation, diamond particles will absorb on the interlayer, which has a positive effect on diamond nucleation. But activated carbon atoms will also diffuse into the tungsten interlayer because of the defects in sputtered tungsten film (holes, dislocations and grain boundaries). As a result, the concentration of activated carbon will decrease and the nucleation time will be prolonged. Without the seeding step, diamond will not nucleate until the tungsten interlayer is carbonized. In other words, the nucleation of diamond is delayed. Also, we observed the morphology of the nucleation surface of the grown diamond film. The nucleation surface is a layer of high quality, ultra-smooth nanocrystalline diamond film, with an array of tiny roughness peaks. The results of this study are expected to provide guidance to researchers in order to evaluate the effect of tungsten interlayer and help researchers choose interlayers wisely.

2. Experimental details

2.1. Pretreatment of the samples

The substrate used in this work is tungsten substrate with the size of 8 mm × 8 mm × 4 mm. First, the polished substrates were washed with alcohol and acetone in ultrasonic bath for 10 min. Then, the substrates were cleaned with a Kauffman ion gun in order to eliminate contaminants and adsorbed gas molecules. The applied voltage was 70 V, with 1.25 A current. The coil current was 6 A, whereas the acceleration voltage and current was set to 500 V and 40 mA, respectively. The gas source was Ar and the pressure in the vacuum chamber was 0.05 Pa. The beam operation voltage was 1.5 kV and beam current was kept at 78 mA.

After ion cleaning for 30 min, the tungsten interlayer was prepared by the DC magnetron sputtering technique in a high vacuum chamber with base pressure < 10⁻⁴ Pa. The purity of the tungsten target and the purity of the argon gas were 99.99 wt.% and 99.99 vol.%, respectively. Pure tungsten thin film was sputtered with sputtering voltage of 350 V and current of 0.4 A. The sputtering pressure of the pure tungsten thin film was kept at 1.0 Pa and sputtering time was 30 min. The target-substrate distance was 70 mm. 300 °C was chosen in order to optimize the adhesion and deposition rate of tungsten thin film.

2.2. Diamond deposition

The diamond films were grown by hot filament assisted CVD in a multifunctional vapor deposition system specifically designed for diamond deposition. The reactor is a stainless steel chamber with an inner diameter of 300 mm to which various electrical, gas and liquid feeds are fitted, as well as a magnetron cathode for sputtering. A spiral

coil tungsten filament is used to activate the gas for diamond film deposition. The filament temperature (T_f) was measured by an optical pyrometer. The reaction gas was a mixture of H₂ and CH₄. The flow rate of H₂ and CH₄ was controlled by mass flow controller (MFC). Substrate surface temperature (T_s) was measured by a K-type thermocouple. The experiment conditions are listed in Table 1. In this table, the samples are divided into six groups to investigate the influence of interlayer (i), methane concentration (M, Mi), pressure (P), temperature (T), reaction time (t) and pretreatment process (Pr).

2.3. Characterization of the samples

Samples were characterized by field-emission scanning electron microscopy (FE-SEM FEI, Sirion200) to reveal the surface morphology of the diamond film. Raman spectroscopy (LabRAM ARAMIS) was employed to characterize the quality and bonding structures of diamond film. The wavelength of the laser is 532 nm with a typical resolution of 1–2 cm⁻¹ in the back-scattering geometry. The diameter of the laser spot is 2 μm. The phases in the samples were analyzed by X-ray Diffraction (XRD, Dmax-2500VBX using Cu Kα radiation at a wavelength of 0.154 nm). Focused ion beam (FEI Helios X600, Interface Analysis Centre, University of Bristol) was applied to illustrate the cross-section morphology of the sample.

3. Experiment results

3.1. Seeding process

Samples i1, i2, i3 and i4 aim to investigate the influence of interlayer and diamond seeding step on nucleation stage of diamond growth. The SEM results are shown in Fig. 1. It is evident that the nucleation density is different for substrate with and without tungsten interlayer. The nucleation density is in the following order: i3 < i1 < i2 < i4. For tungsten block substrates, it is difficult for them to form a continuous diamond film within 180 min, whether or not the substrate was ultrasonically abraded by micro-sized diamond, as shown in Fig. 1 (a, b) and (c, d). However, for i4, which was ultrasonically agitated in diamond slurry, after deposition for 20 min, nanocrystalline diamond film grew continuously on the surface. For i3, diamond only nucleated at defect places, such as scratches, craves and gaps. On an intact surface of tungsten film, diamond can hardly nucleate in such short period of time. The nucleation density of i3 was much lower than that of i1. In Fig. 1 (f), diamond nuclei are observed near the cleft because the energy of the surface near the cleft was higher than non-defect places and diamond is prone to nucleate near those defects [31]. Fig. S1 (a, b) further proved this assumption. In Fig. 1 (h), diamond mainly nucleated on the bottom of the hole, where sputtered tungsten film was peeled off. In Raman patterns, it is clear that the signal–noise ratio of i4 is much better than i3. The peak located at 1150 cm⁻¹ is the Raman peak of transpolyacetylene and it cannot be observed in the Raman pattern of i3. The results of samples i1, i2, i3, and i4 indicated that the nucleation and growth of diamond on sputtered tungsten coating were different from those on sintered tungsten block because the reaction activity of sputtered tungsten is much higher than sintered tungsten. Therefore, the effect of different conditions on diamond film grown on sputtered tungsten coating was investigated in detail.

3.2. Methane concentration

Fig. 2 compared the surface morphology, cross-section morphology and XRD patterns of samples M1, M2 and M3. These samples were sintered tungsten substrate without diamond seeding step. In Fig. 2 (a, d, g), there are four phases in all three samples, that is WC, diamond, tungsten and carbon. XRD results show that as methane concentration increases, the WC layer thickness decreases. The thickness of diamond and WC layers was relatively small and XRD ray can penetrate

Table 1
Detailed experimental conditions and complete list of samples.

Groups	Interlayer				Methane concentration								Pressure			Temperature		Time		Pretreatment	
	i1	i2	i3	i4	M1	M2	M3	Mi1	Mi2	Mi3	Mi4	Mi5	P1	P2	P3	T1	T2	t1	t2	Pr1	Pr2
Sample	i1	i2	i3	i4	M1	M2	M3	Mi1	Mi2	Mi3	Mi4	Mi5	P1	P2	P3	T1	T2	t1	t2	Pr1	Pr2
Substrate	SW		PW		SW			PW					PW			PW		PW		PW	
CH ₄ %	3				1	3	5	1	2	3	4	5	2			2		1		3	
T _s /°C	700				700								700			700	800	700		700	
t/min	20				180								240			180		180	240	180	
P/kPa	3.0				3.0								1.5	3.0	6.0	3.0		3.0		3.0	
Seeding	N	Y	N	Y	N								N			N		N		N	Y

Note: SW: sintered tungsten block substrate PW: PVD sputtered tungsten film. Samples numbered T1 and Mi2, t1 and Mi1, Pr1 and Mi3 are the same.

through these layers. FIB images show that as methane concentration increase, the thickness of diamond film increased from 1 μm at 1% to 3 μm at 5%. The carbide layer cannot be observed because the carbide layer is too thin, which shows that the surface of sintered tungsten blocks can hardly be carbonized. In SEM images, when methane concentration reached 3% and 5%, continuous diamond film can be prepared on non-diamond-pretreated tungsten substrate. As methane concentration dropped to 1%, a few pin holes appeared on the surface, allowing the activated carbon atoms to react with the substrate directly. When methane concentration is higher, a dense diamond film will form on the surface of the substrate in the initial stage of growth. Fig. 2 (j–M3, k–M3, l–M3) provides information about the cross-section of M3. In Fig. 2(j), the crystal surface of diamond film was presented. This proves that the growth of HFCVD diamond film follows the columnar growth model. At the interface of diamond and tungsten substrate, the carbonized layer was revealed because the etching rate among diamond, tungsten and carbonized tungsten is different. At 5% methane concentration, the thickness of diamond layer reached about 3 μm and the thickness of the carbonized tungsten layer was about 150 nm.

The surface morphology and Raman spectroscopy of sample Mi1 to Mi5 were presented in Fig. 3. When methane concentration was 1%, the nucleation density of diamond was very low and the size of diamond grain was approximately 2 μm . The probable reason is that sputtered tungsten film absorbed and reacted with activated carbon clusters and transformed into tungsten carbides. So the density of activated carbon atoms was low near the surface. As methane concentration rose to 3%, the diamond nucleation density increased dramatically. However, the average size of diamond grain decreased, from 7.1 μm (2%) to 4.8 μm (3%). This is because when nucleation density of diamond is high, the space for grain growth is small and the growth of grain will be confined by other grains. Another reason is that higher nucleation density will consume more carbon clusters near the surface and reduce the density of activated carbon atoms. From Fig. 3 (I–III), the diamond peak was sharp and high, which means that the C sp³ content of the deposited film was high. However, non-diamond peaks appeared and the intensity of these peaks became stronger when methane concentration went up to 3%. The result illustrates that methane concentration plays a decisive role in diamond quality at the beginning

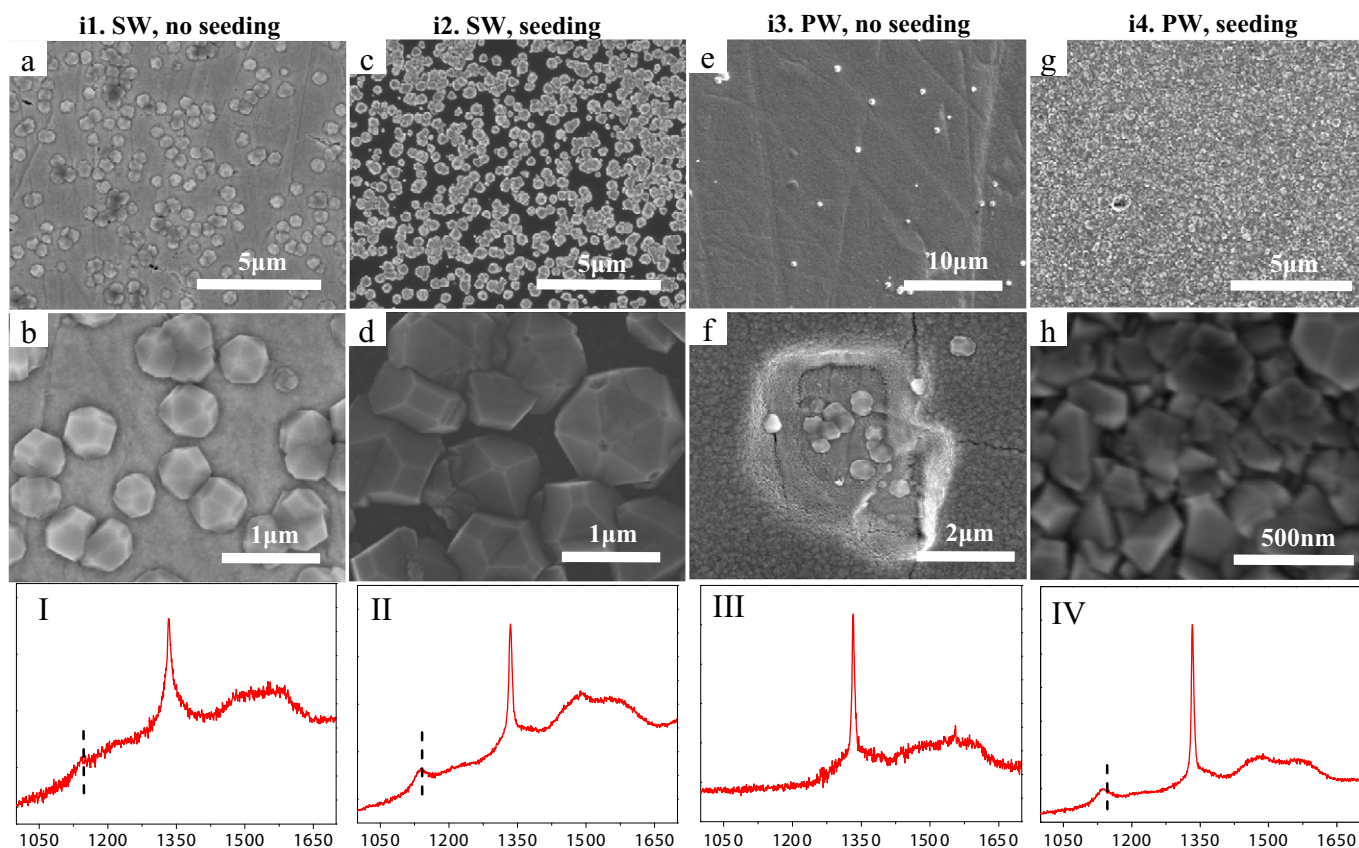


Fig. 1. Representative SEM images and Raman spectra of CVD diamond deposited on specimens i1 (a, b, I), i2 (c, d, II), i3 (e, f, III) and i4 (g, h, IV). Experiment condition: CH₄: 3%, T_s: 700 °C, deposition time: 20 min, pressure: 3 kPa.

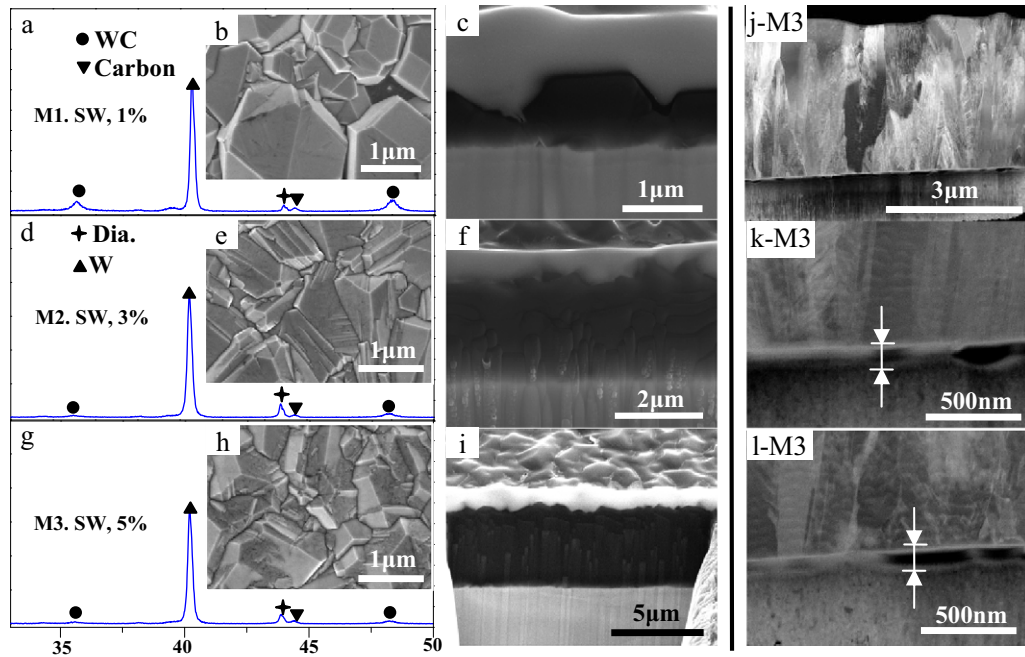


Fig. 2. XRD patterns, SEM images and FIB images of sample M1 (a, b, c), M2 (d, e, f) and M3 (g, h, i), STEM images of the cross-section morphology of sample M3 (j-M3, k-M3, l-M3). Experiment condition: T_s : 700 °C, deposition time: 180 min, pressure: 3 kPa, without seeding process.

stage of diamond nucleation. Lower methane concentration leads to better diamond quality. As methane content in the reaction chamber continued to increase, the nucleation density decreased rapidly at 4% and remained steady at 5%. The diameter of the grain, however, increased all the way up to roughly 10 μm at 5%. SEM images showed

that the surface of diamond grain is smooth under low methane concentration condition. As methane concentration increased, the secondary-nucleation of diamond on the crystal surface increased dramatically and the shape of diamond grain turned into sphere [32]. In Fig. 3 (IV–V), the diamond peaks of Mi4 and Mi5 cannot be observed

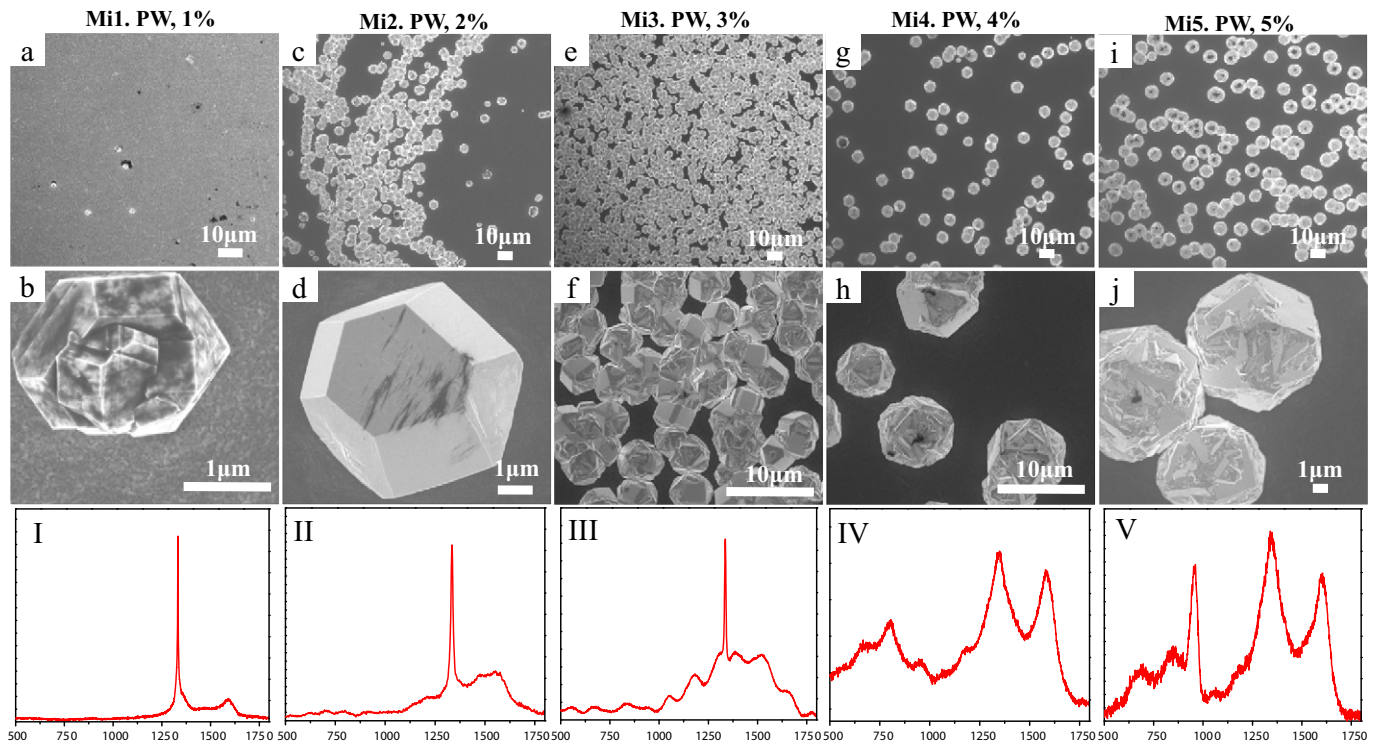


Fig. 3. Representative SEM images and Raman spectra of CVD diamond deposited on specimens Mi1 (a, b, I), Mi2 (c, d, II), Mi3 (e, f, III), Mi4 (g, h, IV) and Mi5 (i, j, V). Experiment condition: T_s : 700 °C, deposition time: 180 min, pressure: 3 kPa, without seeding process.

because they were overlapped by the strong D-peak of sp^2 carbon. At high methane concentration, sp^2 carbon phase was more evident. Also, the peaks located at 660, 810 and 960 cm^{-1} , which were not so strong in previous Raman patterns, were obvious in both figures. These peaks were found in WC thin film prepared by magnetron controlled sputtering as well [33].

Fig. 4 (a–c) is the XRD pattern of sample Mi1, Mi3 and Mi5, respectively. Overall, except the figure for sample Mi1, in which no diamond peak can be found, the peaks existed in each graph were almost the same. As methane concentration increased from 1% to 5%, WC, W_2C and W existed in all samples. In tungsten–carbon binary phase diagram, α -WC is the only stable phase under equilibrium condition. β - W_2C and β - WC_{1-x} will not form unless temperature reaches 1250 °C and 2500 °C, respectively. From the W–C phase diagram, the solubility of carbon in pure tungsten is very small. The maximum value of carbon solubility is 0.7 at.% at 2700 °C. Furthermore, the solubility of carbon decreased rapidly when temperature had a downward trend. Below 500 °C, the dissolved carbon in tungsten can be neglected. β - W_2C is hexagonal structure and carbon atoms were filled in the interval of octahedral structure (tightly packed AAA sequence layer of W). Under different temperature, W_2C has three different phases: β - W_2C , β' - W_2C , β'' - W_2C , which are distinguished by the different locations of carbon atoms in the interval of octahedral structure. The structure of β - WC_{1-x} is similar to NaCl. In many reports, β - WC_{1-x} is predominate phase when preparing W–C film using CVD or PVD technology [34,35]. The grain of prepared β - WC_{1-x} phase is nanocrystalline and sometimes it is amorphous [36]. WC is hexagonal structure and the interval of triangular prism of tungsten atom lattice is filled by carbon atoms. Therefore, the structure of WC is stable and it is easy to form under equilibrium condition. However, it is very difficult to prepare pure hexagonal α -WC using CVD or PVD technology because these technologies are performed under unstable conditions. Therefore, the interlayer after diamond deposition consists of WC, W_2C and WC_{1-x} .

The reason led to the large differences among Raman patterns is that the permeable depth of Raman laser is much smaller than that of X-ray. Variation of methane distribution on the surface during deposition results in different phases on the surface of the film. The peaks located at 660 and 810 cm^{-1} are associated to the bands of WC stretching modes [34,37]. The peak at 960 cm^{-1} is usually assigned to the stretching mode of W=O double bonds that appear on the boundaries of amorphous or nanostructure tungsten oxides [38–41]. The unexpected tungsten oxides may be brought by the residual oxygen in the PVD chamber. Also, the surface of sputtered tungsten layer has high activity, with rich grain boundaries and defects. The sputtered tungsten layer

consists of tungsten nanoparticles, which is highly activated and prone to react with other species. Therefore, the surface of tungsten film will be oxidized during the transferring from PVD chamber to HFCVD reactor. Consequently, the interlayer contains oxidized tungsten impurity.

3.3. Pressure

As deposition pressure increased from 1.4 kPa to 6 kPa, the morphology of SEM and Raman spectroscopy changed significantly. In Fig. 5(a), interspaces between diamond grains can be clearly observed. For sample P2, the deposited diamond film was continuous, while in sample P3, the nucleation density of diamond decreased dramatically and a number of nanosized diamond particles just nucleated on the surface. Raman spectrum of sample P1 and sample P2 were almost the same, while Raman pattern of sample P3 was quite different. In Fig. 5(I) and Fig. 5 (II), the pattern was typical CVD diamond film pattern, which consists of a sharp, strong peak at 1332 cm^{-1} nearby and a wide, weak peak near 1550 cm^{-1} . In Fig. 5 (III), no diamond grains were probed by the Raman laser and two strong peaks located at 660, 810 cm^{-1} nearby can be spotted easily. From XRD patterns in Fig. 6 (a–c), the intensity of W_2C peak was in the following order: P1 < P3 < P2. The result shows that lower pressure is beneficial to the process of carbonization. When pressure in the reaction chamber is higher, the mean free path of activated carbon is shorter. It is easier for the activated carbon atoms to collide with other atoms and recombine into stable molecules. Therefore, less activated carbon atoms are able to reach the surface of the substrate and the content of W_2C is higher. At 3 kPa, nucleation rate and density were high and continuous diamond film was prepared. The seamless diamond film separated activated carbon atoms from the interlayer. Therefore, even though the pressure of sample P2 was lower than that of sample P3, the amount of W_2C is higher than that of sample P3.

3.4. Temperature

When substrate temperature rose to 800 °C, without seeding step, only a few diamond grains nucleated on the sputtered tungsten film after deposition for 180 min, as shown in Fig. 7. Compared with SEM image of sample T1 (Fig. 3 (c, d)), the nucleation density dropped dramatically. Bigger diamond grains reached approximately 6 μm in diameter, while other grains were still below 1 μm in diameter. The intensity of Raman spectroscopy was very low (about 400 at the peak) and signal-to-noise ratio was poor. Compared with sample T1 (Fig. 3 (II)), the ratio of diamond peak and non-diamond peak of sample T2 was much lower. The result showed that higher temperature led to lower diamond nucleation density, which was contrary to the regular regulation of preparing diamond on tungsten blocks. The reason was that the diffusion of carbon atoms in sputtered tungsten film was much faster than in tungsten bulks. As temperature increased, the quantity of carbon atoms diffused into the film increased significantly, which greatly reduced the density of carbon atoms on the surface. Thus the stage of diamond nucleation was prolonged. Also, at higher temperature, carbon atoms were prone to react with tungsten atoms. At 700 °C for 180 min, the reaction produced both W_2C and WC. The W_2C in the film further reacted with carbon and transformed into WC at 800 °C. As we observed from XRD results, when deposition temperature raised up to 800 °C, after 180 min of deposition, the whole tungsten film transformed into WC, while W_2C peak can hardly be observed. The XRD pattern proved that higher temperature led to greater reactive activity of the interlayer. Tungsten was more likely to transform into WC under higher temperature because the activation energy required to produce WC was higher than that of W_2C .

3.5. Deposition time

Fig. 8 showed the surface morphology and XRD pattern of sample t2. As deposition time extended to 240 min, compared with sample t1

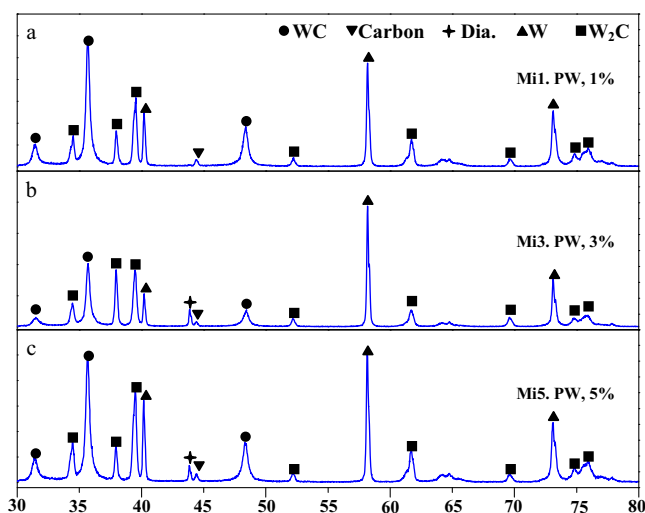


Fig. 4. XRD patterns of (a) sample Mi1, 1%, (b) sample Mi3, 3% and (c) sample Mi5, 5%.

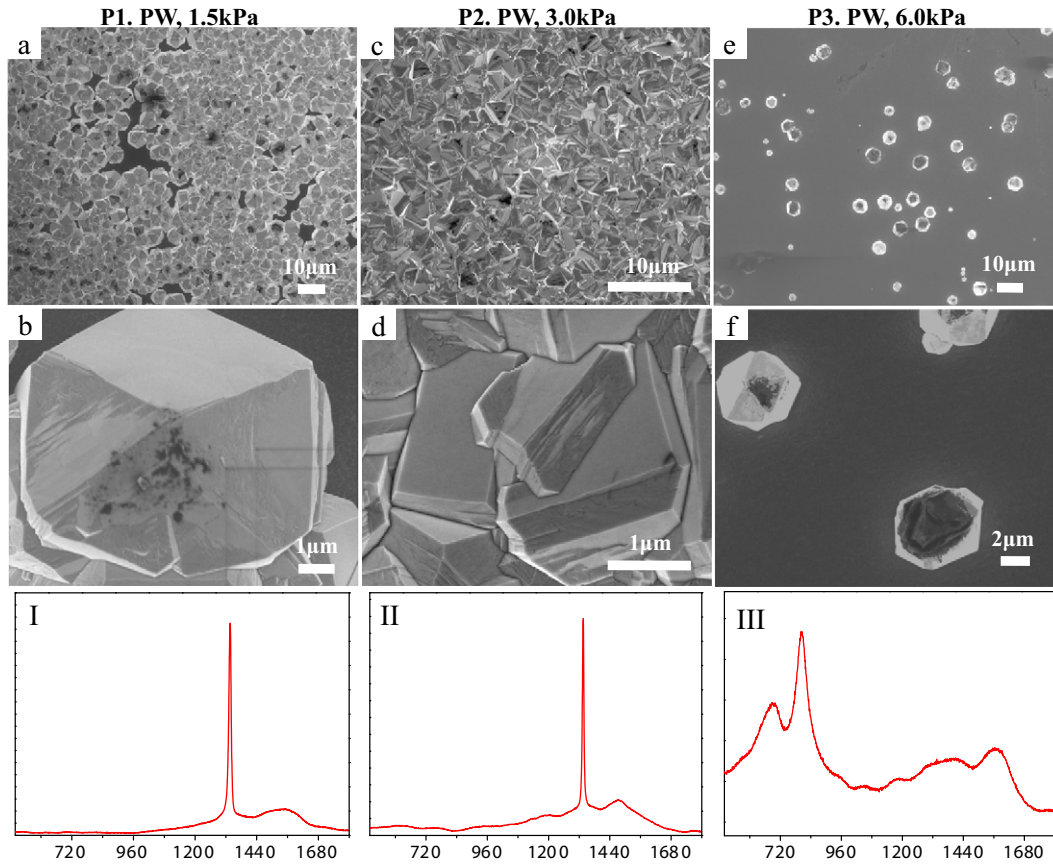


Fig. 5. SEM images and Raman spectra of sample P1 (a, b, I), P2 (c, d, II) and P3 (e, f, III). Experiment condition: CH₄: 2%, T_s: 700 °C, deposition time: 240 min, without seeding step.

(Fig. 3 (a, b)), the number of diamond grains on the tungsten film surface was much bigger. The size of diamond grains varies greatly. Some of the grains were more than 2 μm in diameter, while a considerable number of small grains, less than 200 nm in diameter, were dispersed over the film. The result indicates that the nucleation process is not synchronized. In Fig. 8 (b–f), various shapes of diamond grains were presented. It is recognized that the surface free energy plays a critical role

in determining the shape of a crystal. The surface free energy (γ_{hkl}) of the hkl facet of diamond grain is given by

$$\gamma_{hkl} = \frac{\lambda}{\sqrt{h^2 + k^2 + l^2}} \frac{3E}{8d_0^2}. \quad (1)$$

In Eq. (1), E and d_0 are carbon–carbon bonding energy and bond length of diamond crystal, respectively. λ represents the maximum value of h , k and l . Therefore, the surface free energy of different diamond facets obeys the following formula $\gamma_{100}:\gamma_{110}:\gamma_{111} = 1:\frac{1}{\sqrt{2}}:\frac{1}{\sqrt{3}}$. According to the theory of Gibbs, the equilibrium shape of diamond should be an octahedral crystal with eight (111) surfaces. However, in most of reports, five-symmetric faceted diamond is the predominant production after HFCVD treatment. The result shows that the nucleation process of diamond is not an equilibrium process. Compared with Fig. 4(a), the peaks shown in Fig. 8(g) are similar except that the intensity diamond peak in Fig. 8(g) was more obvious and WC peaks were stronger. The result is in accordance with our previous observation. When the surface of the substrate is not covered by diamond film, under longer reaction time, more W₂C will transform to WC and more diamond grains will nucleate on the surface.

3.6. Nucleation surface

The surface morphology and XRD pattern of sample Pr2, which was agitated in diamond slurry and deposited for 180 min, were presented in Fig. 9. In panel (a), the prepared diamond film grew continuously on the surface and the facets of diamond grains after were clear. The quality of diamond was very good and the size of diamond grain was more than 2 μm. When the sample was taken out from PVD chamber

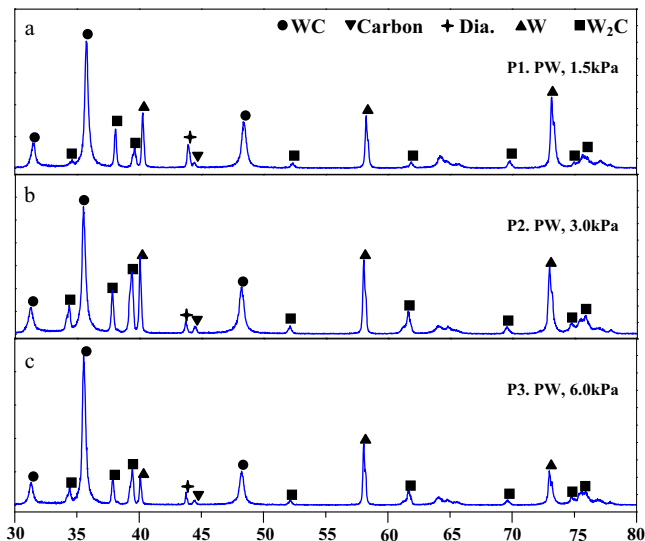


Fig. 6. XRD patterns of (a) sample P1, (b) sample P2 and (c) sample P3.

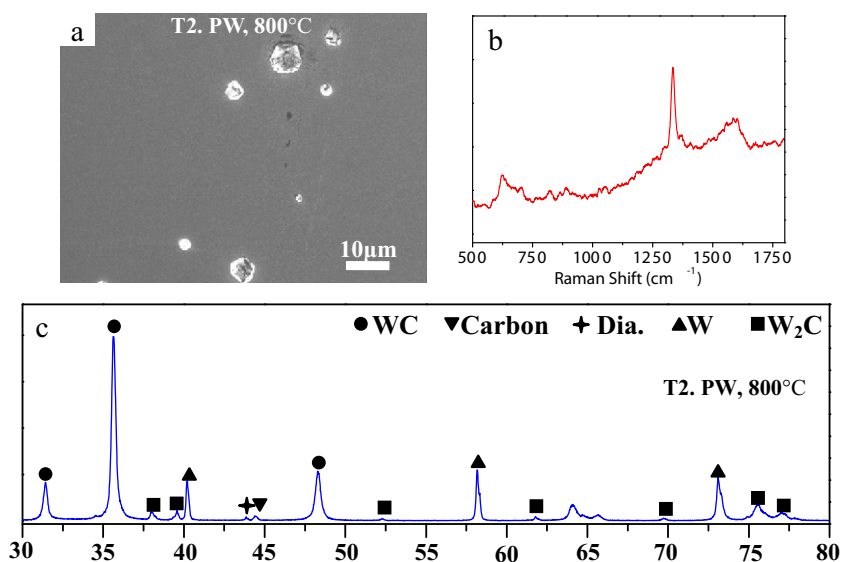


Fig. 7. (a–c) SEM, Raman spectrum and XRD pattern of sample T2. Experiment condition: CH₄: 2%, deposition time: 180 min, pressure: 3 kPa, without seeding step.

and sent to HFCVD reaction chamber after the seeding step, part of sputtered tungsten film was accidentally scratched by tweezers. Panel (b) revealed the morphology of the scratched places after diamond deposition. Fig. 9(c) was the magnification of part 1, in which carbonized interlayer and tungsten substrate were clearly demonstrated. The scratch on original tungsten substrate can be easily observed and the thickness of the diamond film was approximately 2 μm, which can be estimated from the cross-section of diamond film. Also, the thickness of tungsten layer can be estimated, about 1.5 μm in thickness. Panel (h) further illustrated the morphology of the carbonized interlayer shown in picture (c). The top of the interlayer was covered by

nanoparticles, whose diameter was less than 100 nm. Figure (d) was the magnification of part 2 in panel (b). From this figure, it is clear that diamond can grow continuously on the curved tungsten film. In Figure (e), diamond film grows continuously on both sides of the curved tungsten film, showing that diamond can nucleate on the tungsten film easily after the seeding step. Judged from the relative intensity of peaks in the XRD pattern (panel (i)), the main phase of the interlayer was W₂C. Compared with XRD patterns of samples without diamond pre-treatment (sample Pr1, Fig. 4(b)), the WC peak intensity of XRD pattern of sample Pr2 was much weaker than sample Pr1. The result suggested that the seeding step curbed the formation of WC during diamond

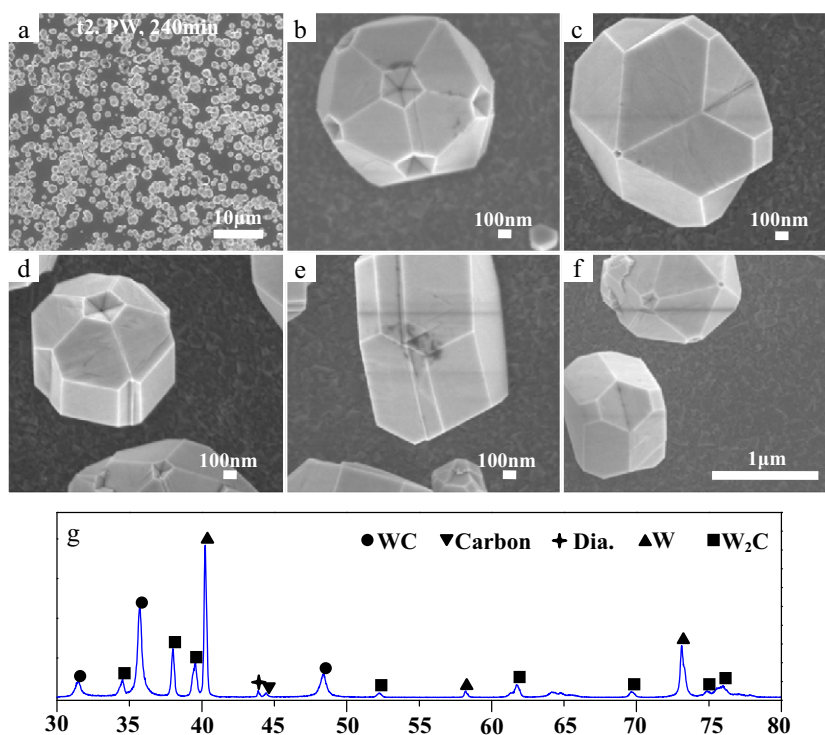


Fig. 8. (a) surface morphology of sample t2 (b–f) different shapes of deposited diamond grains (g) XRD pattern of sample 17. Experiment condition: CH₄: 1%, T_s: 700 °C, pressure: 3 kPa, without seeding step.

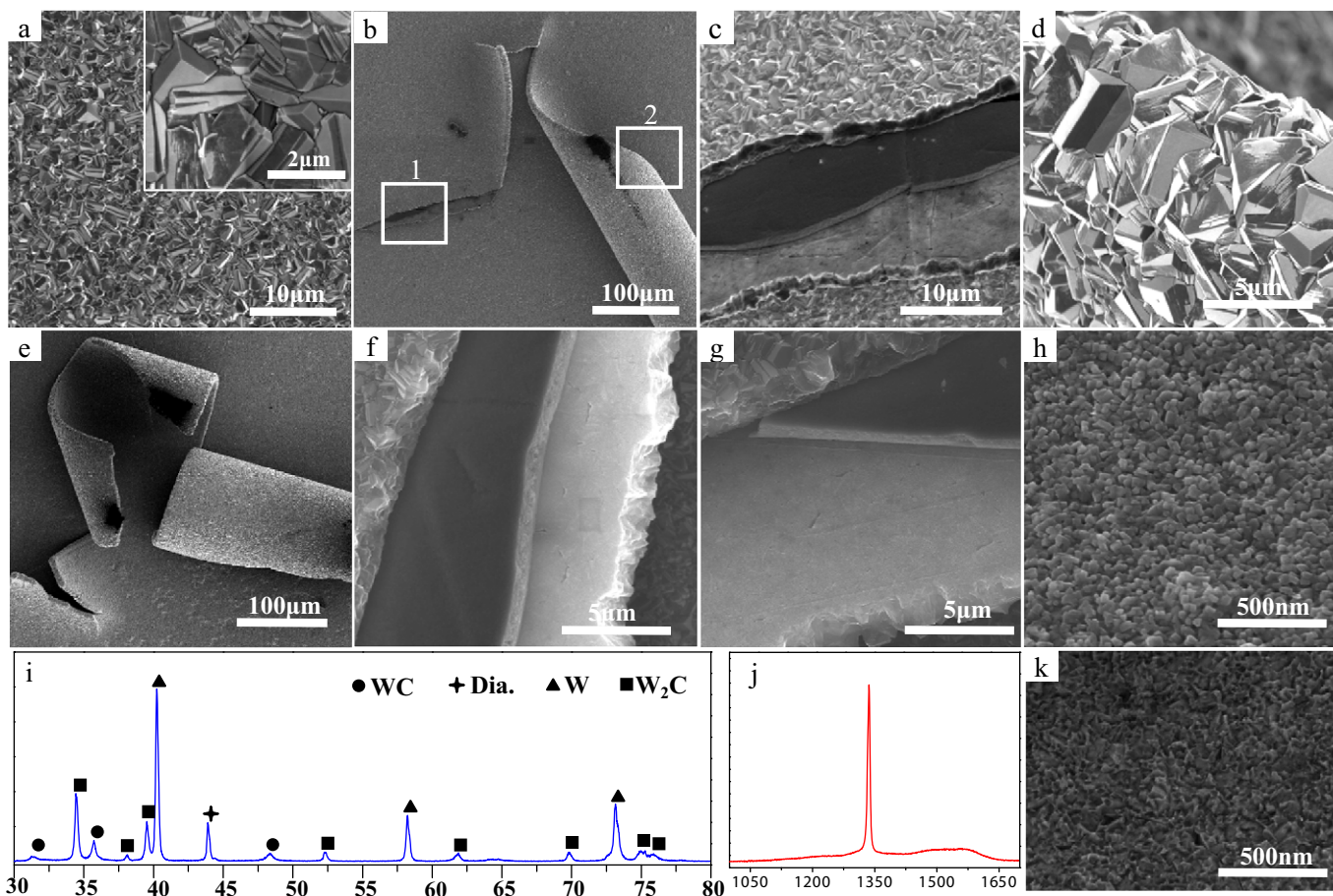


Fig. 9. (a) SEM image of diamond surface morphology of sample Pr2 (b, e) SEM images of scratched film (c) SEM magnification image of part 1 (d) SEM magnification image of part 2 (f, g) SEM images of diamond-interlayer-diamond multilayer film (h) surface morphology of the carbonized tungsten interlayer (i) XRD pattern of sample Pr2 (j) Raman spectrum of nucleation surface of diamond film (k) surface morphology of the nucleation side of diamond film. Experiment condition: CH_4 : 3%, T_s : 700 °C, deposition time: 180 min, pressure: 3 kPa.

deposition because the pretreatment process greatly increased the nucleation density and the nucleated diamond grew into continuous diamond film in less than 20 min. The continuous diamond film blocked the activated carbon atoms from the interlayer. As a result, the amount of WC dropped rapidly. So the formation of WC in sputtered tungsten film during HFCVD diamond process has two steps. The first one is that tungsten film must be fully carbonized into W_2C because carbon-poor phases (W_2C) are more likely to form. The second step is that reactive carbon atoms should be transported on the surface of the film to further carbonize the interlayer after the first step.

In Fig. 9 (f, g, k), the nucleation surface of diamond film was clearly presented. The interlayer was sandwiched by two diamond films. The reason led to this peculiar morphology is described as follows. After the PVD tungsten process, the sample was transferred into CVD reaction chamber by tweezers and part of the tungsten film was scratched by them. The scratched tungsten film rolled up and during diamond deposition and diamond film grows at both side of the interlayer. At cooling stage, due to the mismatch in thermal expansion coefficient, part of diamond film and carbonized tungsten film peeled off from the multilayer film. Therefore, the nucleation surface of diamond revealed. The magnification of the nucleation surface presents the subtle micro-architecture of nucleation surface. On the whole, the surface is seamless, except some clefts caused by thermal expansion. The nucleation surface is covered by small hemisphere holes with tiny peaks at the edges of each hole. This architecture may have many applications, such as field emission and MEMS [42–45]. In Fig. 9(j), diamond peak is very sharp and the intensity other than non- sp^3 carbon peaks is very weak, which indicate that the quality of diamond is much better compared

with the beginning stage of nucleation, shown in Fig. 1 (IV). The reason is that as deposition time prolonged, the sp^2 carbon formed at the beginning stage of nucleation diffuses into the interlayer. The diffusion behavior of sp^2 carbon reduced the amount of impurities along the grain boundary thus enhanced the quality of diamond film. Through this modulation effect of PVD tungsten layer, the quality of diamond can be changed to meet different requirements.

4. Discussion

As shown in the previous section, the surface reactivity of the substrates poses large influence on the nucleation density of diamond. For diamond films grown on substrates with high surface reactivity, many research articles have proved that the nucleation density of diamond film will be greatly enhanced after the seeding process [30,31]. Continuous, ultrasoft and nanocrystalline diamond film can be prepared within a short period of time. In this paper, we found that once the PVD tungsten coated substrates were not ultrasonically agitated by diamond dispersion, the nucleation density will be lower than the diamond nucleation density on sintered tungsten substrates. We figure that unlike Ti substrate, on which the nucleation of diamond does not depend on the formation of carbide layer [46], the nucleation of diamond films on tungsten substrate is closely related to the carbonization of the substrates and surface concentration of carbon cluster. On sintered tungsten substrates, the thickness of diffusion layer is limited. However, on PVD tungsten film, entire PVD tungsten film will be carbonized before diamond nucleation. Next, we focus on the diffusion behavior of carbon in PVD tungsten film.

4.1. The diffusion behavior of carbon in PVD tungsten film

For sintered tungsten block substrate, the diffusion depth of carbon in the substrate is limited and the diffusion layer is mainly composed of tungsten carbide. The diffusion of carbon in sintered tungsten substrate is concentration dependent [47]. However, the diffusion depth of carbon in PVD tungsten interlayer is much larger and the diffusion layer consists of WC and W_2C . The amount of tungsten converted to WC and W_2C during HFCVD is determined by methane concentration, surface coverage of diamond, pressure, temperature and deposition time. Methane concentration mainly affects the density of activated carbon atoms in the reaction chamber. As methane concentration increases, the density of activated carbon atoms increases, which should result in increasing of carbides in the interlayer. However, surface coverage of diamond film also plays a critical role in determining the carbonization of interlayer. Diamond film will block the active carbon atoms from the interlayer. Therefore, with an increase of surface coverage of diamond, carbonization of interlayer will be curbed. Lower pressure is beneficial to the process of carbonization. When pressure in the reaction chamber is higher, the mean free path of activated carbon is shorter. It is easier for the activated carbon atoms to collide with other atoms and recombine into stable molecules. Therefore, less activated carbon atoms are able to reach the surface of the substrate. As temperature increases, carbon moves faster in the interlayer. In addition, the activation energy of WC formation is higher than W_2C . As a result, after 180 min of HFCVD at 800 °C, the interlayer was almost carbonized into WC.

4.2. Diamond nucleation surface

It is very difficult for researchers to prepare smooth diamond film on tungsten blocks because of surface replication effect and uneven island nucleation and growth. On sintered tungsten blocks, continuous diamond film requires a long time to deposit and the surface will become rugged because of the crystal surface of the micro-sized diamond grains. After the seeding step, diamond film can grow continuously on the surface of sputtered tungsten film within 20 min. The result shows that sputtered tungsten film having a high surface reactivity. In the ultrasonic vibration process of nanodiamond acetone suspension, the surface of sputtered W film can absorb large amounts of nanodiamond seeds, thereby greatly increasing the nucleation density of CVD diamond. Therefore, the sputtered tungsten film can be regarded as a candidate for preparing ultrasmooth nanocrystalline diamond film. However, the quality of the diamond film is rather low and there is sp^2 carbon phase in the grain boundary. From Fig. 9(j), it is obvious that the diamond quality of nucleation surface is rather high. After diamond grow continuous on sputtered tungsten film in a short time (<20 min), the tungsten film is not completely carbonized. The continuous diamond film serve as a barrier for activated carbon atoms to react with tungsten film and the sp^2 carbon formed at the grain boundary will diffuse into the tungsten film. As a result, the quality of diamond at the nucleation surface is greatly improved. Based on this, a new method, including an etching process, is introduced. First tungsten is sputtered on tungsten foil substrate by sputtering technology. Tungsten foil is used to reduce the cost of the process. After diamond pretreatment, diamond film is deposited on the surface. After that, by etching tungsten foil and PVD tungsten film using acid or Murakami reagent, the nucleation surface of diamond film can be obtained. In fact, we have been using this technique for preparing ultra-smooth self-supporting diamond film. We have tried to grow diamond film directly on polished silicon substrate and then etching the silicon substrate in order to obtain the nucleation surface of diamond. However, on the nucleation surface, there are large holes because of the uneven island nucleation. Using sputtered tungsten film can avoid such problem. Because of low thermal expansion mismatch between tungsten and diamond, this can become a new method to prepare high-quality and ultra-smooth nanocrystalline freestanding diamond film with special surface morphology.

5. Conclusions

The influence of parameters can be concluded as follows:

1. Lower pressure is beneficial to the process of carbonization.
2. As a result of continuous carbon uptake, the PVD tungsten film transforms in the following order: $W_2C / WC_{1-x} / WC(C\text{-supersaturated}) / WC + \text{diamond}$.

The use of a PVD tungsten film has two opposite effects. First, after diamond powder ultrasonic bath, the tungsten film will adsorb a large number of diamond nanoparticles. Therefore, the nucleation density of diamond will be substantially improved. The other effect is that the film will be carbonized during deposition process and carbon concentration on the surface of the film will decrease. The carbonization process can be concluded as follows. During HFCVD deposition, methane is activated by the high temperature filament and activated carbon atoms are produced when methane decomposed. Then carbon atoms react with the tungsten layer, which transforms into W_2C in the first place. When the whole PVD layer became W_2C , diamond begins to nucleate on the defected spot on the surface, which has higher surface energy. At the same time, graphite and other non- sp^3 carbon formed on the surface of the film. As the deposition process proceeds, sp^2 carbon diffuses into the PVD layer and reacts with W_2C , from which WC phase is produced. The interlayer after diamond deposition consists of oxidized tungsten, WC, W_2C and WC_{1-x} .

The nucleation surface of diamond was revealed at the scratched part of the tungsten film. The nucleation surface is ultrasmooth and seamless nanocrystalline diamond with high-quality and special surface architecture (tiny peaks arrays). This can be a good way to produce field-emission devices and MEMS devices based on diamond.

Prime novelty statement

We deposited the diamond film on sintered tungsten substrates and PVD tungsten film substrates, and investigated the diffusion behavior of carbon in tungsten film under various deposition conditions. We confirm that this paper is our original, unpublished work that has not been submitted to any other journal for review.

Supplementary data to this article can be found online at <http://dx.doi.org/10.1016/j.diamond.2014.12.009>.

Acknowledgments

We thank Prof. Mike Ashfold in Department of Chemistry, University of Bristol for his instruction. We also thank Prof. Tom Scott and Dr. Scott Greenwell in Interface Analysis Center, University of Bristol for their help in FIB and STEM test. We gratefully acknowledge the National Natural Science Foundation of China (No.51301211 & No.21271188), the China Postdoctoral Science Foundation (No.2012M521541), the Fundamental Research Funds for the Central Universities (No.2012QNZT002), the State Key Laboratory of Powder Metallurgy (No.20110933K), and the Open-End Fund for Valuable and Precision instruments of Central South University (No.CSU2013016) for financial support.

References

- [1] G.A. Slack, Thermal conductivity of pure and impure silicon, silicon carbide, and diamond, *J. Appl. Phys.* 35 (1964) 3460.
- [2] P.W. May, The new diamond age? *Science* 319 (2008) 1490.
- [3] H. Sein, W. Ahmed, C.A. Rego, A.N. Jones, M. Amar, M. Jackson, R. Polini, Chemical vapour deposition diamond coating on tungsten carbide dental cutting tools, *J. Phys. Condens. Matter* 15 (2003) S2961.
- [4] H. Sein, W. Ahmed, M. Jackson, R. Woodwards, R. Polini, Performance and characterisation of CVD diamond coated, sintered diamond and WC-Co cutting tools for dental and micro machining applications, *Thin Solid Films* 447–448 (2004) 455.
- [5] D.F. Marc, K.V. Yogesh, Nanostructured diamond film deposition on curved surfaces of metallic temporomandibular joint implant, *J. Phys. D. Appl. Phys.* 35 (2002) L105.
- [6] C.O. Townley, Diamond Coated Joint Implant, Google Patents, 2003.

- [7] J.E. Graebner, S. Jin, G.W. Kammlott, J.A. Herb, C.F. Gardinier, Unusually high thermal conductivity in diamond films, *Appl. Phys. Lett.* 60 (1992) 1576.
- [8] Y. Yamamoto, T. Imai, K. Tanabe, T. Tsuno, Y. Kumazawa, N. Fujimori, The measurement of thermal properties of diamond, *Diam. Relat. Mater.* 6 (1997) 1057.
- [9] C. Wang, A. Garcia, D.C. Ingram, M. Lake, M.E. Kordeš, Cold field emission from CVD diamond films observed in emission electron microscopy, *Electron. Lett.* 27 (1991) 1459.
- [10] O. Auciello, et al., Are diamonds a MEMS' best friend? *Microw. Mag. IEEE* 8 (2007) 61.
- [11] O. Auciello, A.V. Sumant, Status review of the science and technology of ultrananocrystalline diamond (UNCD™) films and application to multifunctional devices, *Diam. Relat. Mater.* 19 (2010) 699.
- [12] H. Liu, D.S. Dandy, Studies on nucleation process in diamond CVD: an overview of recent developments, *Diam. Relat. Mater.* 4 (1995) 1173.
- [13] J.H. Luong, K.B. Male, J.D. Glennon, Boron-doped diamond electrode: synthesis, characterization, functionalization and analytical applications, *Analyst* 134 (2009) 1965.
- [14] B.V. Sarada, T.N. Rao, D.A. Tryk, A. Fujishima, Electrochemical characterization of highly boron-doped diamond microelectrodes in aqueous electrolyte, *J. Electrochem. Soc.* 146 (1999) 1469.
- [15] A. Suzuki, T.A. Ivandini, K. Yoshimi, A. Fujishima, G. Oyama, T. Nakazato, N. Hattori, S. Kitazawa, Y. Einaga, Fabrication, characterization, and application of boron-doped diamond microelectrodes for in vivo dopamine detection, *Anal. Chem.* 79 (2007) 8608.
- [16] P.W. May, C.A. Rego, R.M. Thomas, M.N.R. Ashfold, K.N. Rosser, N.M. Everitt, CVD diamond wires and tubes, *Diam. Relat. Mater.* 3 (1994) 810.
- [17] P.W. May, C.A. Rego, R.M. Thomas, M.N.R. Ashfold, K.N. Rosser, P.G. Partridge, N.M. Everitt, Preparation of solid and hollow diamond fibres and the potential for diamond fibre metal matrix composites, *J. Mater. Sci. Lett.* 13 (1994) 247.
- [18] V. Baranauskas, H.J. Ceraglioli, A.C. Peterlevitz, Fabrication of tubes of diamond with micrometric diameters and their characterization, *Thin Solid Films* 420–421 (2002) 151.
- [19] S. Silva, M.C. Salvadori, K. Kawakita, M.T. Pereira, W. Rossi, M. Cattani, Fabrication of diamond flow controller micronozzles, *Diam. Relat. Mater.* 11 (2002) 237.
- [20] S. Silva, M.C. Salvadori, K. Kawakita, M.T. Pereira, R.M. Galvão, M. Cattani, Diamond flow controller microtubes, *J. Micromech. Microeng.* 12 (2002) 108.
- [21] Q. Wei, Z.M. Yu, M.N.R. Ashfold, Z. Chen, L. Wang, L. Ma, Effects of thickness and cycle parameters on fretting wear behavior of CVD diamond coatings on steel substrates, *Surf. Coat. Technol.* 205 (2010) 158.
- [22] J.P. Manaud, A. Poulon, S. Gomez, Y.L. Petitcorps, A comparative study of CrN, ZrN, NbN and TaN layers as cobalt diffusion barriers for CVD diamond deposition on WC–Co tools, *Surf. Coat. Technol.* 202 (2007) 222.
- [23] J.G. Buijnsters, P. Shankar, W. Fleischer, W.J.P. van Enckevort, J.J. Schermer, J.J. ter Meulen, CVD diamond deposition on steel using arc-plated chromium nitride interlayers, *Diam. Relat. Mater.* 11 (2002) 536.
- [24] K. Vandierendonck, M. Nesládek, S. Kadlec, C. Quaeysaegens, M. Van Stappen, L.M.M. Stals, W/WC diffusion barrier layers for CVD diamond coatings deposited on WC–Co: microstructure and properties, *Surf. Coat. Technol.* 98 (1998) 1060.
- [25] N.N. Naguib, et al., Enhanced nucleation, smoothness and conformality of ultrananocrystalline diamond (UNCD) ultrathin films via tungsten interlayers, *Chem. Phys. Lett.* 430 (2006) 345.
- [26] J.G. Buijnsters, J.-P. Celis, R.W.A. Hendrikx, L. Vázquez, Metallic seed nanolayers for enhanced nucleation of nanocrystalline diamond thin films, *J. Phys. Chem. C* 117 (2013) 23322.
- [27] V.G. Ralchenko, A.A. Smolin, V.G. Pereverzev, E.D. Obratsova, K.G. Korotoushenko, V.I. Konov, Y.V. Lakhotkin, E.N. Loubnin, Diamond deposition on steel with CVD tungsten intermediate layer, *Diam. Relat. Mater.* 4 (1995) 754.
- [28] R. Polini, M. Barletta, G. Rubino, S. Vesco, Recent advances in the deposition of diamond coatings on co-cemented tungsten carbides, *Adv. Mater. Sci. Eng.* 2012 (2012) 14.
- [29] J.G. Buijnsters, L. Vázquez, G. Van Dremel, J. Ter Meulen, W. Van Enckevort, J.-P. Celis, Enhancement of the nucleation of smooth and dense nanocrystalline diamond films by using molybdenum seed layers, *J. Appl. Phys.* 108 (2010) 103514.
- [30] Q. Wei, T. Yang, K. Zhou, L. Ma, P. Zheng, J. Li, D. Zhang, Z. Li, Z. Yu, Effect of sputtered Mo interlayers on Si (100) substrates for the deposition of diamond film by hot filament chemical vapor deposition, *Surf. Coat. Technol.* 232 (2013) 456.
- [31] J.G. Buijnsters, L. Vázquez, J.J. ter Meulen, Substrate pre-treatment by ultrasonication with diamond powder mixtures for nucleation enhancement in diamond film growth, *Diam. Relat. Mater.* 18 (2009) 1239.
- [32] H. Zhuang, X. Jiang, Growth controlling of diamond and β -SiC microcrystals in the diamond/ β -SiC composite films, *Surf. Coat. Technol.* 249 (2014) 84.
- [33] Q. Wei, Z. Yu, L. Ma, D. Yin, Enhanced nucleation and smoothness of nanocrystalline diamond films via W–C gradient interlayer, *Int. J. Mod. Phys. B* 23 (2009) 1676.
- [34] S.E. Mrabet, M.D. Abad, C. López-Cartes, D. Martínez-Martínez, J.C. Sánchez-López, Thermal evolution of WC/C nanostructured coatings by Raman and in situ XRD analysis, *Plasma Process. Polym.* 6 (2009) S444.
- [35] M.D. Abad, M.A. Muñoz-Márquez, S. El Mrabet, A. Justo, J.C. Sánchez-López, Tailored synthesis of nanostructured WC/a–C coatings by dual magnetron sputtering, *Surf. Coat. Technol.* 204 (2010) 3490.
- [36] Q.P. Wei, Z.M. Yu, L. Ma, D.F. Yin, J. Ye, The effects of temperature on nanocrystalline diamond films deposited on WC–13 wt.% Co substrate with W–C gradient layer, *Appl. Surf. Sci.* 256 (2009) 1322.
- [37] B.Q. Yang, X.P. Wang, H.X. Zhang, Z.B. Wang, P.X. Feng, Effect of substrate temperature variation on nanostructured WC films prepared using HFCVD technique, *Mater. Lett.* 62 (2008) 1547.
- [38] C. Bittencourt, R. Landers, E. Llobet, X. Correig, J. Calderer, The role of oxygen partial pressure and annealing temperature on the formation of W=O bonds in thin WO₃ films, *Semicond. Sci. Technol.* 17 (2002) 522.
- [39] G.A. de Wijs, R.A. de Groot, Amorphous WO₃: a first-principles approach, *Electrochim. Acta* 46 (2001) 1989.
- [40] M. Boulova, G. Lucazeau, Crystallite nanosize effect on the structural transitions of wo₃ studied by Raman spectroscopy, *J. Solid State Chem.* 167 (2002) 425.
- [41] A. Baserga, V. Russo, F. Di Fonzo, A. Bailini, D. Cattaneo, C.S. Casari, A. Li Bassi, C.E. Bottani, Nanostructured tungsten oxide with controlled properties: synthesis and Raman characterization, *Thin Solid Films* 515 (2007) 6465.
- [42] J. Robertson, Mechanisms of electron field emission from diamond, diamond-like carbon, and nanostructured carbon, *J. Vac. Sci. Technol. B Microelectron. Nanometer Struct.* 17 (1999) 659.
- [43] J.B. Cui, M. Stammer, J. Ristein, L. Ley, Role of hydrogen on field emission from chemical vapor deposited diamond and nanocrystalline diamond powder, *J. Appl. Phys.* 88 (2000) 3667.
- [44] A.A. Talin, L.S. Pan, K.F. McCarty, T.E. Felter, H.J. Doerr, R.F. Bunshah, The relationship between the spatially resolved field emission characteristics and the Raman spectra of a nanocrystalline diamond cold cathode, *Appl. Phys. Lett.* 69 (1996) 3842.
- [45] K. Wu, E.G. Wang, Z.X. Cao, Z.L. Wang, X. Jiang, Microstructure and its effect on field emission emission of grain-size-controlled nanocrystalline diamond films, *J. Appl. Phys.* 88 (2000) 2967.
- [46] S.S. Park, J.Y. Lee, Synthesis of diamond films on titanium substrates by hot-filament chemical vapor deposition, *J. Appl. Phys.* 69 (1991) 2618.
- [47] K. Schmid, J. Roth, Concentration dependent diffusion of carbon in tungsten, *J. Nucl. Mater.* 302 (2002) 96.